

Pressure Dependence of Fiber Bragg Grating Inscribed in Perfluorinated Polymer Fiber

Ryo Ishikawa, Heeyoung Lee¹, Amédée Lacraz, Antreas Theodosiou², *Student Member, IEEE*,
Kyriacos Kalli, *Member, IEEE*, Yosuke Mizuno¹, *Senior Member, IEEE*,
and Kentaro Nakamura, *Member, IEEE*

Abstract—We investigate the hydrostatic pressure dependence of the Bragg wavelength of a fiber Bragg grating (FBG) inscribed in a perfluorinated graded-index (PFGI-) polymer optical fiber (POF) at 1550 nm. At 0.5 MPa, the Bragg wavelength increased with time and became almost constant ~ 150 min later. Such a long time constant probably originates from the unique structure of the PFGI-POF, which has a thick overcladding around its core and cladding. The pressure-dependence coefficient without considering the time constant was estimated to be 1.3 nm/MPa; this is over five times the values of other types of POF-FBGs. This indicates that by removing the overcladding of the PFGI-POF, fast-response high-sensitivity pressure sensing will be feasible. Once the Bragg wavelength became constant at 0.5 MPa, the pressure-dependence coefficient of the Bragg wavelength was measured to be -0.13 nm/MPa, the absolute value of which was comparable with those of other POF-FBGs, but with an opposite sign.

Index Terms—Polymer optical fibers, fiber Bragg gratings, pressure sensing, temporal variations.

I. INTRODUCTION

OPTICAL fiber sensing techniques have been vigorously studied to perform various physical, chemical, and biological measurements [1], [2]. The sensing configurations are classified into two types: distributed sensing and single- (or multiple-) point sensing. The former includes strain and/or temperature sensing based on Brillouin scattering [3]–[5]; although the distributed measurement capability is a great advantage, its sensitivity is not sufficiently high for some applications (such as small-strain detection of $\ll 10 \mu\epsilon$). The latter includes sensing based on fiber Bragg gratings (FBGs) [6]–[15], the sensitivity of which is generally higher than that of the former at the cost of the limited number of sensing points. Here, we focus on FBG sensors.

Manuscript received October 10, 2017; revised October 20, 2017; accepted October 24, 2017. Date of publication October 27, 2017; date of current version November 10, 2017. This work was supported in part by JSPS KAKENHI under Grant 17H04930 and Grant 17J07226, in part by the Japan Gas Association, in part by the ESPEC Foundation for Global Environment Research and Technology, and in part by the Association for Disaster Prevention Research. (*Corresponding author: Yosuke Mizuno.*)

R. Ishikawa, H. Lee, Y. Mizuno, and K. Nakamura are with the Institute of Innovative Research, Tokyo Institute of Technology, Yokohama 226-8503, Japan (e-mail: rishikawa@sonic.pi.titech.ac.jp; hylee@sonic.pi.titech.ac.jp; ymizuno@sonic.pi.titech.ac.jp; knakamur@sonic.pi.titech.ac.jp).

A. Lacraz, A. Theodosiou, and K. Kalli are with the Nanophotonics Research Laboratory, Cyprus University of Technology, Limassol 3036, Cyprus (e-mail: amedee.lacraz@cut.ac.cy; theodosiou.antreas@gmail.com; kyriacos.kalli@cut.ac.cy).

Color versions of one or more of the figures in this letter are available online at <http://ieeexplore.ieee.org>.

Digital Object Identifier 10.1109/LPT.2017.2767082

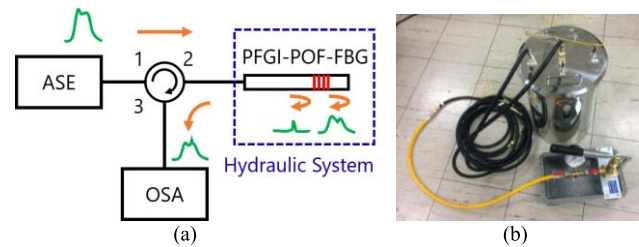


Fig. 1. (a) Experimental setup. ASE: amplified spontaneous emission; OSA: optical spectrum analyzer. (b) Photograph of hydraulic system.

The interest in using FBGs as point sensors is limited not only to strain and temperature [8] but to humidity [9], refractive index [10], and many other physical parameters. In particular, pressure sensing is one of the major targets, and a number of relevant results have been reported using FBGs inscribed in glass optical fibers [11]–[15]. As the intrinsic pressure sensitivity of the FBG in glass fibers is relatively small [15], higher-sensitivity pressure sensing has been basically achieved by converting pressure into strain [11]–[14]. In the meantime, as polymeric materials are generally softer than glass materials, intrinsic pressure sensitivities have been enhanced using FBGs inscribed in some types of polymer optical fibers (POFs) [16]–[18]. For instance, at telecom wavelengths, FBGs in a single-mode (SM-) poly(methyl methacrylate) (PMMA-) POF [16] and a multimode microstructured (MM-m) POF [17] are reported to have pressure sensitivities of ~ 0.25 nm/MPa (corresponding to a fractional sensitivity (Bragg wavelength shift divided by the initial Bragg wavelength for fair comparison) of $\sim 163 \times 10^{-6}$ /MPa) and ~ 0.1 nm/MPa (corresponding to $\sim 64 \times 10^{-6}$ /MPa), respectively, the absolute values of which are approximately ~ 82 and ~ 32 times larger than the typical value of an FBG in a silica single-mode fiber (SMF) (-3.1 pm/MPa, corresponding to -2.0×10^{-6} /MPa) [15]. However, such conventional POF-FBGs suffer from extremely high propagation loss at 1550 nm.

There is interest in the use of perfluorinated graded-index (PFGI-) POFs, which have been developed for short distance communication systems (relatively low propagation loss even at 1550 nm) [19]. The PFGI-POFs are only available as multimode fibers and are not photosensitive in the UV wavelength region; both these issues have complicated the FBG inscription. Recently, some research groups have developed inscription techniques for FBGs in PFGI-POFs [20]–[23].

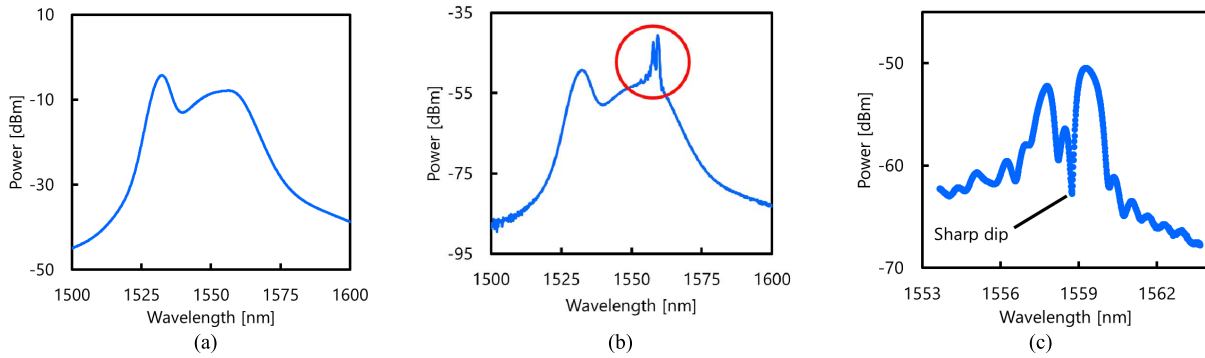


Fig. 2. (a, b) Measured optical spectra of the ASE output and the reflected light, respectively. (c) Magnified view of the red-circled part in (b), around the FBG-induced peaks.

At 1550 nm, amplified spontaneous emission (ASE) can be directly used as a wideband light source for interrogating the Bragg wavelength. Moreover, the core refractive index of PFGI-POF-FBGs is close to that of water, which is beneficial for bio-sensing applications [24]. To date, the strain, temperature, and humidity sensing characteristics of PFGI-POF-FBGs have been investigated [20], [25], [26], but no reports have been provided regarding their pressure dependence.

In this work, at 1550 nm, we investigate the hydrostatic pressure dependence of the Bragg wavelength of a PFGI-POF-FBG for the first time to the best of our knowledge.

II. FBG INSCRIPTION AND MEASUREMENT SETUP

A 2-mm-long FBG was inscribed in a 1.3-m-long PFGI-POF. The PFGI-POF (GigaPOF-50SR, Chromis Fiberoptics) has a three-layered structure: core (diameter: 50 μm ; refractive index: ~ 1.35), cladding (diameter: 70 μm , refractive index: ~ 1.34), and overcladding (diameter: 490 μm). The core and cladding consist of doped and undoped amorphous fluoropolymer (CYTOP®), respectively, the water absorption of which is negligibly small [27], and the overcladding is composed of polycarbonate. The optical propagation loss is relatively low (~ 0.25 dB/m) even at 1550 nm. The numerical aperture was ~ 0.19 . The FBG was inscribed without removal of the overcladding using a femtosecond laser system (High Q femtoREGEN, High Q Laser) operating at 517 nm with a pulse duration of 220 fs. The laser was operated at a repetition rate of 1 kHz, for a pulse energy of ~ 100 nJ [20], [28]. The PFGI-POF was mounted on an air bearing translation system (Aerotech); this allowed high-resolution and high-accuracy motion on two axes. A long working distance objective (x50) was mounted on a third axis, and the laser beam was focused into the fiber. Accurate synchronization of the laser pulse repetition rate and the stage motion allowed for plane-by-plane grating inscription, enabling the grating to have a desired length and an index-modulation value [20], [22], [23], [28].

Figure 1(a) shows an experimental setup for measuring the Bragg wavelength of the FBG. All the optical paths except the PFGI-POF were silica SMFs. The output from an ASE source was injected into the PFGI-POF, and the reflected light from the FBG was guided via an optical circulator to an optical spectrum analyser (AQ6370, Yokogawa Electric Corp.;

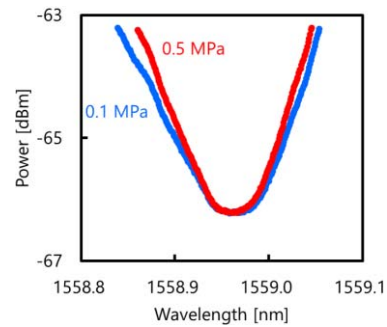


Fig. 3. FBG-reflected spectra around the sharp dip measured at 0.1 MPa (blue) and 0.5 MPa (red).

stability: ± 0.02 nm in the range from 1520 to 1580 nm; reproducibility: ± 0.005 nm in 1 min). We employed a reflectometric (not transmissive) configuration to minimize the influence of modal interference [29]. The PFGI-POF was placed in a hydraulic system (MN151-001, Think-Lands; Fig. 1(b)), in which the hydrostatic pressure P can be controlled from 0.1 MPa (atmospheric pressure) to 0.5 MPa. One end of the PFGI-POF was connected to a silica SMF using a so-called butt-coupling technique (SMF-to-POF coupling loss: ~ 0.2 dB; theoretical returning loss: -28 dB) [30], and the other end was kept open. Note that the Fresnel reflection at the open end is automatically suppressed because the refractive index of water is ~ 1.33 , close to that of the fiber core (~ 1.35).

III. EXPERIMENTAL RESULTS

We first measured the optical spectra of the ASE output and the FBG-reflected light, as shown in Figs. 2(a) and (b). The spectrum of the light Fresnel-reflected mainly at the SMF-to-POF boundary was overlapped with the FBG-reflected spectrum, which was still clearly observed at 1559 nm. The magnified view of the FBG-reflected spectrum around its peaks is shown in Fig. 2(c). Multiple peaks and dips, caused by the multimode nature of the POF [31], were observed in the spectrum. The wavelength of any peak or dip (including the highest peak) could be selected as a Bragg wavelength, but here, the clear and sharpest dip at 1558.97 nm was used to enhance the measurement accuracy.

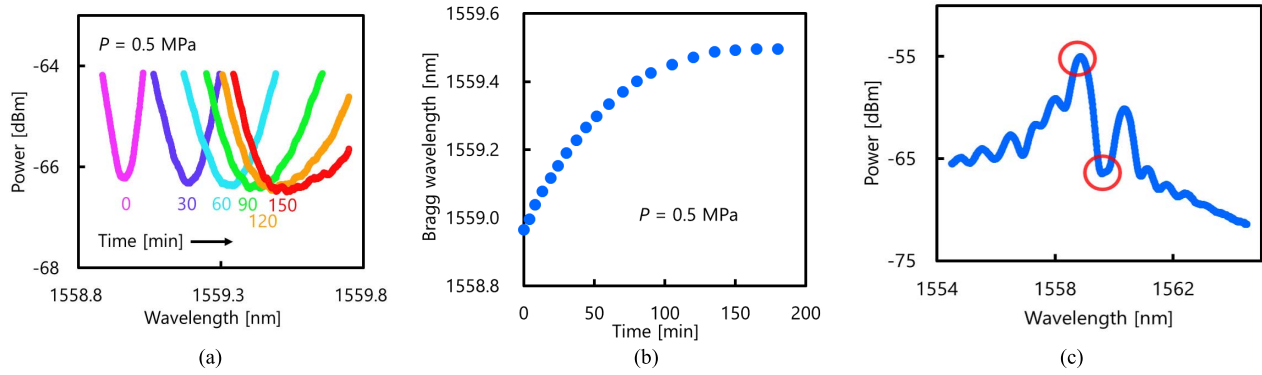


Fig. 4. (a) Temporal dependence of the FBG-reflected spectrum at 0.5 MPa. (b) Temporal dependence of the Bragg wavelength at 0.5 MPa. (c) FBG-reflected spectrum measured after 0.5-MPa pressure was applied for 240 min. The red-circled parts are the dip (right) and the peak (left) used in measurements.

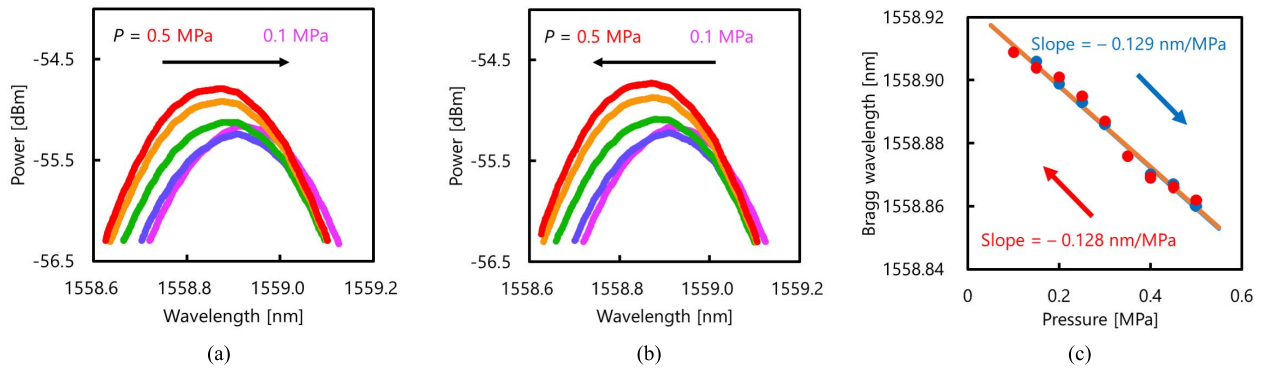


Fig. 5. (a, b) Pressure dependences of FBG-induced spectra around the sharp peak when the pressure was decreased from 0.5 MPa to 0.1 MPa and when the pressure was then increased from 0.1 MPa to 0.5 MPa. (c) Measured Bragg wavelength dependence on pressure; the red points indicate the data when the pressure was decreased, and the blue points are the data when the pressure was then increased. The two lines are their linear fits, which are overlapped and appear to be one line in this figure.

Subsequently, we measured the FBG-reflected spectra around the dip before and after the pressure P was abruptly (within 20 s) increased from 0.1 MPa (atmospheric) to 0.5 MPa, as shown in Fig. 3. Although the linewidth of the dip was slightly reduced, the Bragg wavelength shift was negligibly small. After that, however, as the pressure P was maintained at 0.5 MPa, the Bragg wavelength shifted as time proceeded, as shown in Fig. 4(a). Figure 4(b) shows the temporal dependence of the Bragg wavelength at 0.5 MPa. The Bragg wavelength increased with time and, approximately 150 min later became almost constant. The total Bragg wavelength shift was approximately 0.5 nm. The positive dependence of the Bragg wavelength on pressure was the same as those of other types of POFs [16], [17], but the wavelength shift accompanying a time constant of over several tens of minutes was first observed in this measurement. Such a long time constant appears to be caused by the structure of the PFGI-POF, which is composed of two different polymer materials (CYTOP (core and cladding; pressure strength: 30 MPa) is known to be mechanically much weaker than polycarbonate (overcladding; pressure strength: 86 MPa)). If we consider that the Bragg wavelength dependence on pressure without considering the time constant (i.e., when the Bragg wavelength is measured at each pressure after waiting for a

sufficiently long time for the signal to be constant) is linear, the dependence coefficient is estimated to be ~ 1.3 nm/MPa (corresponding to $\sim 860 \times 10^{-6}$ /MPa). This value is ~ 5.2 and ~ 13 times larger than those of the FBGs in an SM-PMMA-POF [16] and MM-mPOF [17], respectively. This result indicates that, by removing the overcladding of the PFGI-POF in advance, higher-sensitivity pressure sensing with a short response time could be achieved. Note that the linewidth of the dip increased with time, and compared with Fig. 2(c), the FBG-reflected spectrum was so much changed (Fig. 4(c)) that the dip was no longer sharp, therefore we used the highest peak for the following measurements.

Finally, the pressure dependence of the Bragg wavelength (measured using the highest peak, as mentioned above) was measured in a short period (< 1 min). Figures 5(a) and (b) show the pressure dependences of the FBG-reflected spectra when the pressure P was decreased from 0.5 MPa to 0.1 MPa and when P was then increased from 0.1 MPa to 0.5 MPa, respectively. In both cases, as the pressure became higher, the Bragg wavelength grew shorter. The spectral power change seems to have been caused by the multimode nature of the POF. The Bragg wavelength was then plotted as a function of pressure P , as shown in Fig. 5(c). Irrespective of the direction of the pressure change, the Bragg wavelength

exhibited a negative dependence on pressure with a coefficient of -0.13 nm/MPa (standard deviation: <2.72 pm; corresponding to a fractional sensitivity of -84×10^{-6} /MPa). This absolute value is ~ 42 , ~ 0.52 , and ~ 1.3 times larger than those of the FBGs in a silica SMF [15], SM-PMMA-POF [16], and MM-mPOF [17], respectively. The negative dependence, which is opposite to those of other types of POFs [16], [17], is caused by the fact that the contribution of the elongated grating pitch is greater than that of the reduced refractive index in this short-term measurement. The drawing-induced anisotropy [17], [32] and three-layered structure of the PFGI-POF may need to be considered for further analysis. The imperfectly linear pressure dependence of the Bragg wavelength probably originates from the multimode nature of the POF, but as long as the dependence is monotonic, it can be used to perform pressure sensing by exploiting the one-to-one correspondence between the Bragg wavelength and pressure.

IV. CONCLUSION

The hydrostatic pressure dependence of the Bragg wavelength of an FBG inscribed in a PFGI-POF was investigated at 1550 nm. The Bragg wavelength shift was negligibly small shortly after the pressure was abruptly increased to 0.5 MPa. However, when the FBG was maintained at 0.5 MPa, the Bragg wavelength increased with time and became almost constant ~ 150 min later. The long time constant seems to have been caused by the overcladding. A simply calculated pressure-dependence coefficient was 1.3 nm/MPa, which is more than 5 times the values of other types of POF-FBGs. The pressure-dependence coefficient was measured at -0.13 nm/MPa. Unlike other POF-FBGs, the sign of the pressure-dependence coefficient was negative while the absolute value was not significantly different. Our results may indicate the feasibility of high-sensitivity pressure sensing with a short response time by removing the overcladding of the PFGI-POF-FBG.

REFERENCES

- [1] L. S. Grattan and B. T. Meggitt, *Optical Fiber Sensor Technology Advanced Applications—Bragg Gratings and Distributed Sensors*. Dordrecht, The Netherlands: Springer, 2000.
- [2] A. H. Hartog, *An Introduction to Distributed Optical Fibre Sensors*. Boca Raton, FL, USA: CRC Press, 2017.
- [3] T. Horiguchi and M. Tateda, "BOTDA-nondestructive measurement of single-mode optical fiber attenuation characteristics using Brillouin interaction: Theory," *J. Lightw. Technol.*, vol. 7, no. 8, pp. 1170–1176, Aug. 1989.
- [4] K. Hotate and T. Hasegawa, "Measurement of Brillouin gain spectrum distribution along an optical fiber using a correlation-based technique—Proposal, experiment and simulation," *IEICE Trans. Electron.*, vols. E83–C, no. 3, pp. 405–412, 2000.
- [5] Y. Mizuno, N. Hayashi, H. Fukuda, K. Y. Song, and K. Nakamura, "Ultrahigh-speed distributed Brillouin reflectometry," *Light, Sci. Appl.*, vol. 5, p. e16184, Dec. 2016.
- [6] R. Kashyap, *Fiber Bragg Gratings*. San Diego, CA, USA: Elsevier, 1999.
- [7] A. Othonos and K. Kalli, *Fiber Bragg Gratings: Fundamentals and Applications in Telecommunications and Sensing*. Boston, MA, USA: Artech House, 1996.
- [8] F. Farahi, D. J. Webb, J. D. C. Jones, and D. A. Jackson, "Simultaneous measurement of temperature and strain: Cross-sensitivity considerations," *J. Lightw. Technol.*, vol. 8, no. 2, pp. 138–142, Feb. 1990.
- [9] P. Kronenberg, P. K. Rastogi, P. Giaccari, and H. G. Limberger, "Relative humidity sensor with optical fiber Bragg gratings," *Opt. Lett.*, vol. 27, no. 16, pp. 1385–1387, 2002.
- [10] A. Iadicicco, A. Cusano, A. Cutolo, R. Bernini, and M. Giordano, "Thinned fiber Bragg gratings as high sensitivity refractive index sensor," *IEEE Photon. Technol. Lett.*, vol. 16, no. 4, pp. 1149–1151, Apr. 2004.
- [11] W. T. Zhang, F. Li, Y. L. Liu, and L. H. Liu, "Ultrathin FBG pressure sensor with enhanced responsivity," *IEEE Photon. Technol. Lett.*, vol. 19, no. 19, pp. 1553–1555, Oct. 1, 2007.
- [12] D. Sengupta and P. Kishore, "Continuous liquid level monitoring sensor system using fiber Bragg grating," *Opt. Eng.*, vol. 53, no. 1, p. 017102, 2014.
- [13] H.-J. Sheng, M.-Y. Fu, T.-C. Chen, W.-F. Liu, and S.-S. Bor, "A lateral pressure sensor using a fiber Bragg grating," *IEEE Photon. Technol. Lett.*, vol. 16, no. 4, pp. 1146–1148, Apr. 2004.
- [14] Y. Zhang *et al.*, "High-sensitivity pressure sensor using a shielded polymer-coated fiber Bragg grating," *IEEE Photon. Technol. Lett.*, vol. 13, no. 6, pp. 618–619, Jun. 2001.
- [15] M. G. Xu, L. Reekie, Y. T. Chow, and J. P. Dakin, "Optical in-fibre grating high pressure sensor," *Electron. Lett.*, vol. 29, no. 4, pp. 398–399, 1993.
- [16] K. Bhowmik *et al.*, "Experimental study and analysis of hydrostatic pressure sensitivity of polymer fibre Bragg gratings," *J. Lightw. Technol.*, vol. 33, no. 12, pp. 2456–2462, Jun. 15, 2015.
- [17] I. P. Johnson, D. J. Webb, and K. Kalli, "Hydrostatic pressure sensing using a polymer optical fibre Bragg gratings," *Proc. SPIE*, vol. 8351, p. 835106, Jan. 2012.
- [18] R. A. Furukawa, A. Tagaya, and Y. Koike, "Pressure measurement based on a multimode phase retarder plastic optical fiber," *ACS Appl. Mater. Interfaces*, vol. 1, no. 3, pp. 720–725, 2009.
- [19] Y. Koike and M. Asai, "The future of plastic optical fiber," *NPG Asia Mater.*, vol. 1, no. 1, pp. 22–28, Oct. 2009.
- [20] A. Lacraz, M. Polis, A. Theodosiou, C. Koutsides, and K. Kalli, "Femtosecond laser inscribed Bragg gratings in low loss CYTOP polymer optical fiber," *IEEE Photon. Technol. Lett.*, vol. 27, no. 7, pp. 693–696, Apr. 1, 2015.
- [21] M. Koerdt *et al.*, "Fabrication and characterization of Bragg gratings in a graded-index perfluorinated polymer optical fiber," *Proc. Technol.*, vol. 15, pp. 138–146, Oct. 2014.
- [22] A. Theodosiou, M. Polis, A. Lacraz, K. Kalli, M. Komodromos, and A. Stassis, "Comparative study of multimode CYTOP graded index and single-mode silica fibre Bragg grating array for the mode shape capturing of a free-free metal beam," *Proc. SPIE*, vol. 9886, p. 98860O, Apr. 2016.
- [23] A. Lacraz, A. Theodosiou, and K. Kalli, "Femtosecond laser inscribed Bragg grating arrays in long lengths of polymer optical fibres; a route to practical sensing with POF," *Electron. Lett.*, vol. 52, no. 19, pp. 1626–1627, 2016.
- [24] G. Zhou, C.-F. J. Pun, H.-Y. Tam, A. C. L. Wong, C. Lu, and P. K. A. Wai, "Single-mode perfluorinated polymer optical fibers with refractive index of 1.34 for biomedical applications," *IEEE Photon. Technol. Lett.*, vol. 22, no. 2, pp. 106–108, Jan. 15, 2010.
- [25] P. Stajanca, A. Lacraz, K. Kalli, M. Schukar, and K. Krebber, "Strain sensing with femtosecond inscribed FBGs in perfluorinated polymer optical fibers," *Proc. SPIE*, vol. 9899, p. 989911, Apr. 2016.
- [26] A. Theodosiou, M. Komodromos, and K. Kalli, "Accurate and fast demodulation algorithm for multipeak FBG reflection spectra using a combination of cross correlation and Hilbert transformation," *J. Lightw. Technol.*, vol. 35, no. 18, pp. 3956–3962, Sep. 15, 2017.
- [27] S. Ando, T. Matsuura, and S. Sasaki, "Perfluorinated polymers for optical waveguides," *Chemtech*, vol. 24, pp. 20–27, Dec. 1994.
- [28] A. Theodosiou *et al.*, "Modified fs-laser inscribed FBG array for rapid mode shape capture of free-free vibrating beams," *IEEE Photon. Technol. Lett.*, vol. 28, no. 14, pp. 1509–1512, Jul. 15, 2016.
- [29] T. Kawa, G. Numata, H. Lee, N. Hayashi, Y. Mizuno, and K. Nakamura, "Single-end-access strain and temperature sensing based on multimodal interference in polymer optical fibers," *IEICE Electron. Exp.*, vol. 14, no. 3, p. 20161239, 2017.
- [30] Y. Mizuno and K. Nakamura, "Experimental study of Brillouin scattering in perfluorinated polymer optical fiber at telecommunication wavelength," *Appl. Phys. Lett.*, vol. 97, no. 2, p. 021103, 2010.
- [31] C. Lu and Y. Cui, "Fiber Bragg grating spectra in multimode optical fibers," *J. Lightw. Technol.*, vol. 24, no. 1, pp. 598–604, Jan. 2006.
- [32] K. Peters, "Polymer optical fiber sensors—A review," *Smart Mater. Struct.*, vol. 20, no. 1, p. 013002, 2011.